

surface. The forces measured between these layers do not conform obviously or closely to predictions made for irreversibly adsorbed homopolymer layers immersed in good solvents. On the other hand, a rather simple adaptation of the Alexander–de Gennes theory^{28,29} of terminally attached chains to the case of block copolymers provides a coherent interpretation of our force measurements.

A more complete theory of the $F(D)$ curves, enabling prediction of the magnitude of F at a certain D , will be difficult to accomplish without more detailed knowledge of the configuration of the molecules in the adsorbed layer, via means independent from the inferences we have made here from the surface forces measurement. For example, it is not known from any direct measurement whether, when these two copolymer layers are brought together, the PS chains initially compress or interpenetrate. The very limited lateral mobility of these chains and the step-function-like shape^{28–30} of the segment density profile in these swollen layers of high surface density argue against interpenetration. Direct spectroscopic investigation of the molecular configuration and degree of segmental mixing between the layers when they are brought together would be very valuable to the interpenetration. A photophysical technique such as fluorescence quenching or energy transfer may be useful.

In a more general vein, the application of surface forces measurement between polymer layers has, we believe, great potential to resolve some fundamental problems in adhesion, surface

chemistry, and structured fluids, such as block copolymer–homopolymer blends,^{30,35–37} that exhibit a rich variety of phase behavior.

Acknowledgment. We gratefully acknowledge the contributions of Patricia M. Cotts of IBM to the work of characterizing these copolymers. Financial support of this work at the University of Minnesota was provided by the National Science Foundation, Polymers Program (NSF-DMR 81-15733 and 85-01018), and by an IBM Polymer Fellowship to Sanjay Patel. The work on surface forces at Minnesota owes much to Jacob Israelachvili of the Australian National University, who supervised the construction of our apparatus at ANU and generously assisted us at an early stage in establishing our own measurement capability. In this connection we acknowledge, too, important assistance from Roger Horn and Richard Pashley (ANU). We are grateful to Phil Pincus (UCSB), Jacob Klein (Weizmann Institute), Bill Russel (Princeton), and Pierre-Gilles de Gennes (Collège de France) for critical discussion concerning this work.

Registry No. (PV2P)(PS) (copolymer), 24980-54-9.

Supplementary Material Available: A 3-page description of the experimental technique, including a diagram of the apparatus (Figure A), and three tables including the data of Figures 2–6 (7 pages). Ordering information is given on any current masthead page.

Test of Variational Transition State Theory and Multidimensional Semiclassical Transmission Coefficient Methods against Accurate Quantal Rate Constants for $H + H_2/HD$, $D + H_2$, and $O + H_2/D_2/HD$, Including Intra- and Intermolecular Kinetic Isotope Effects

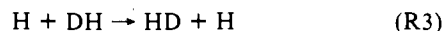
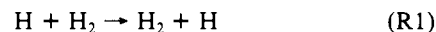
Bruce C. Garrett,[†] Donald G. Truhlar,^{*‡} and George C. Schatz^{*±}

Contribution from the Chemical Dynamics Corporation, Columbus, Ohio 43220, the Department of Chemistry, University of Minnesota, Minneapolis, Minnesota 55455, and the Department of Chemistry, Northwestern University, Evanston, Illinois 60201. Received September 27, 1985

Abstract: Rate constants and kinetic isotope effects for the title reactions have been calculated by using accurate quantum dynamical methods and used to test the accuracy of corresponding rate constants from conventional and variational transition state theory. The quantum dynamical rate constants are estimated to be within 35% of the exact rate constants for the potential surfaces chosen for this comparison. For all the reactions considered, the conventional and variational transition state theory rate constants with unit transmission coefficient are found to be very close to each other (better than 7%) but in poor agreement with the accurate quantum results (off by factors of 6–22 at 300 K). This indicates that although variational effects are small, tunnelling makes a very important contribution to the rate constants, and it is found that this tunnelling contribution is described quantitatively for all the reactions considered with use of the least action ground state (LAG) transmission coefficient. The combination of improved canonical variational theory (ICVT) and LAG yields rate constants which have an average error (considering all the reactions and temperatures studied) of 15% compared to the accurate quantum rate constants, and in only one case ($D + H_2$ at 200 K) does the ICVT/LAG rate constant differ by more than 35% from the accurate value. The comparison of ICVT/LAG kinetic isotope effects is found to be similarly good, with the worst comparisons occurring for intramolecular ($X + HD$) isotope ratios.

I. Introduction

Recent advances in quantal reactive scattering methods have made it possible to calculate rate constants without dynamical approximations for two series of isotopically related reactions:^{1,2}

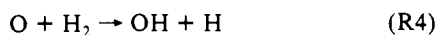


and

[†]Chemical Dynamics Corp.

[‡]University of Minnesota.

[±]Northwestern University.



Although these calculations are subject to errors due to inaccuracies in the assumed potential energy surfaces, the errors due to the numerical treatment of the dynamics are believed to be less than 35%, as discussed below. Therefore these calculations can be used to test the reliability of approximate dynamical methods, provided the approximate calculations are based on the same potential surfaces. In this paper we present such comparisons for variational transition state theory (VTST) with ground-state (G) transmission coefficients (VTST/G).³⁻⁶

VTST calculations are useful for identifying geometric, energetic, and entropic characteristics of dynamical bottlenecks to reaction, and VTST/G calculations are useful for quantitative estimates of reaction rates corresponding to a given potential energy surface and of potential surface barrier heights corresponding to experimental rate data and for the interpretation of kinetic isotope effects.⁷⁻¹⁰ Previously, VTST/G rate constants have been compared with accurate quantal ones for many reactions in a collinear world^{3-6,11,12} but only for three reactions in a three-dimensional world, namely reaction R1¹³ and the reactions¹⁴ $\text{D} + \text{HBr} \rightarrow \text{DBr} + \text{H}$ and $\text{H} + \text{H}'\text{Br} \rightarrow \text{HBr} + \text{H}'$. In each case the comparison involved accurate quantal dynamical rate constants and VTST/G ones for the same assumed potential energy surface. The agreement of accurate and approximate dynamical calculations was quite good for all three systems, with errors of less than 40% at $T \geq 300$ K. An additional check showed that the semiclassical methods used to estimate tunnelling contributions to VTST/G rate constants are also accurate enough to calculate the spectroscopic splitting caused by the inversion of ammonia.¹⁵ Also, VTST/G calculations of the tunnelling contributions for low-temperature surface diffusion of H on Cu lead to excellent agreement with an independent semiclassical estimate.¹⁶

The present comparisons provide more detailed quantitative tests of VTST/G methods, with special focus on deuterium isotope effects at temperatures where tunnelling dominates the dynamics. Although the extensive comparisons of VTST/G results with accurate quantum collinear results noted above are generally very encouraging, they do not test how well VTST/G describes bending

effects on the rate constant. Bending contributions to the energy requirement for reaction play an important quantitative role in determining threshold energies and activation energies,¹⁷ and several approximate methods including the popular quasiclassical trajectory method have been found to describe bending effects very poorly.^{17a} The three-dimensional comparisons of VTST/G and quantum results noted above provide some indication that the VTST/G method describes bending effects accurately, but the present study extends the number of three-dimensional reactions for which such comparisons are available from three to nine, and it thus allows a better assessment of the general applicability of the VTST/G method. Two of the systems considered previously, $\text{D} + \text{HBr}$ and $\text{H} + \text{H}'\text{Br}$, are examples of small curvature reactions where adiabatic theory is expected to do best, while the third, $\text{H} + \text{H}_2$, exhibits greater curvature of the reaction path, but its dynamical bottleneck occurs at a point where the curvature is relatively small. The present comparison considers reactions with a large range of curvatures, bottleneck locations, and bending effects, so the conclusions should be of more general applicability. In addition, the present study is the first test of approximate theory for intramolecular isotope ratios, which are of great experimental interest but whose interpretation involves subtle effects. Intramolecular kinetic isotope effects have never been determined previously at the present level of quantum mechanical sophistication, and the present comparison should enable a clear-cut assessment of how well the VTST/G method describes them.

The accurate quantum rate constants for the present study have been obtained from two different theories. For $\text{H} + \text{H}_2$ and its isotopic variants, rate constants were obtained¹ by using the centrifugal sudden (also called coupled states or CS) approximation¹⁸ for reactive scattering calculations and by using potential surface no. 2 of Porter and Karplus.¹⁹ In these calculations, the Schrödinger equation is solved by a converged CS propagation/matching technique which should yield rate constants which are accurate to at least 35%,²⁰ based on comparisons with close coupling (CC) calculations that represent a converged numerical solution to the nuclear motion Schrödinger equation. The $\text{O} + \text{H}_2$ reaction and its isotopic variants have been studied² by using the CS distorted wave (CSDW) method.²¹ This method introduces the CS approximation in determining the nonreactive wave functions which are used to evaluate the distorted wave approximation²² to the reactive scattering matrix. Past experience with the CSDW approximation indicates that the rate constants obtained should be as accurate as the CS ones (i.e., less than 35% errors) provided that the temperature is low enough so that contributions from energies where the reaction probability is greater than 10% are not important.²¹ The potential surface used for reactions R4-R7 is a modified version of the London-Eyring-Polanyi-Sato-type²³ surface of Johnson and Winter.²⁴ For the present study the potential energy surface used for each system is assumed to represent the true lowest energy potential surface, the reaction is assumed to be electronically adiabatic, and contributions from higher energy surfaces are assumed to be negligible. Since these assumptions are made for both the accurate and approximate dynamics calculations, they do not contribute any error to the tests of VTST/G methods.

In comparison of VTST/G and accurate quantal dynamical results, we will place special emphasis on kinetic isotope effects (KIEs). This is the first opportunity to make systematic tests of

- (1) Schatz, G. C.; Kuppermann, A., to be published.
- (2) Schatz, G. C. *J. Chem. Phys.* **1985**, *83*, 5677.
- (3) Garrett, B. C.; Truhlar, D. G.; Grev, R. S.; Magnuson, A. W. *J. Phys. Chem.* **1980**, *84*, 1730. Errata: *Ibid.* **1983**, *87*, 4554.
- (4) Truhlar, D. G.; Garrett, B. C. *Acc. Chem. Res.* **1980**, *13*, 440.
- (5) Truhlar, D. G.; Isaacson, A. D.; Skodje, R. T.; Garrett, B. C. *J. Phys. Chem.* **1982**, *86*, 2252; **1983**, *87*, 4554 (E).
- (6) Garrett, B. C.; Truhlar, D. G. *J. Chem. Phys.* **1983**, *79*, 4931.
- (7) Rai, S. N.; Truhlar, D. G. *J. Chem. Phys.* **1983**, *79*, 6046. Isaacson, A. D.; Sund, M. T.; Rai, S. N.; Truhlar, D. G. *J. Chem. Phys.* **1985**, *82*, 1338.
- (8) Truhlar, D. G.; Runge, K.; Garrett, B. C. Twentieth International Symposium on Combustion, Combustion Institute, Pittsburgh, 1985; p 585.
- (9) Garrett, B. C.; Truhlar, D. G. *J. Am. Chem. Soc.* **1979**, *101*, 4534, 5207. Garrett, B. C.; Truhlar, D. G.; Grev, R. S. In "Potential Energy Surfaces and Dynamics Calculations"; Truhlar, D. G., Ed.; Plenum: New York, 1981; p 587. Truhlar, D. G.; Garrett, B. C.; Blais, N. C. *J. Chem. Phys.* **1984**, *80*, 232.
- (10) Garrett, B. C.; Truhlar, D. G. *J. Am. Chem. Soc.* **1980**, *102*, 2559. Garrett, B. C.; Truhlar, D. G.; Magnuson, A. W. *J. Chem. Phys.* **1981**, *74*, 1029; **1982**, *76*, 2321. Isaacson, A. D.; Truhlar, D. G. *J. Chem. Phys.* **1982**, *76*, 1380. Truhlar, D. G.; Grev, R. S.; Garrett, B. C. *J. Phys. Chem.* **1983**, *87*, 3415. Tucker, S. C.; Truhlar, D. G.; Garrett, B. C.; Isaacson, A. D. *J. Chem. Phys.* **1985**, *82*, 4102.
- (11) Garrett, B. C.; Truhlar, D. G. *J. Chem. Phys.* **1984**, *81*, 309.
- (12) Truhlar, D. G.; Garrett, B. C. *Annu. Rev. Phys. Chem.* **1984**, *35*, 159. Truhlar, D. G.; Garrett, B. C.; Hipes, P. G.; Kuppermann, A. *J. Chem. Phys.* **1984**, *81*, 3542. Garrett, B. C.; Abusabi, N.; Kouri, D. J.; Truhlar, D. G. *J. Chem. Phys.* **1985**, *83*, 2252.
- (13) Garrett, B. C.; Truhlar, D. G. *Proc. Natl. Acad. Sci. U.S.A.* **1979**, *76*, 4755.
- (14) Clary, D. C.; Garrett, B. C.; Truhlar, D. G. *J. Chem. Phys.* **1983**, *78*, 777. See also: Clary, D. C. *J. Chem. Phys.* **1985**, *83*, 1685.
- (15) Brown, F. B.; Tucker, S. C.; Truhlar, D. G. *J. Chem. Phys.* **1985**, *83*, 4451.
- (16) Lauderdale, J. G.; Truhlar, D. G. *J. Am. Chem. Soc.* **1985**, *107*, 4590.

- (17) For recent examples see: (a) Schatz, G. C. *J. Chem. Phys.* **1983**, *79*, 5386. (b) Steckler, R.; Truhlar, D. G.; Garrett, B. C. *J. Chem. Phys.* **1985**, *83*, 2870.
- (18) Pack, R. T. *J. Chem. Phys.* **1974**, *60*, 633. McGuire, P.; Kouri, D. J. *J. Chem. Phys.* **1974**, *60*, 2488. Kuppermann, A.; Schatz, G. C.; Dwyer, J. P. *Chem. Phys. Lett.* **1977**, *45*, 71.
- (19) Porter, R. N.; Karplus, M. *J. Chem. Phys.* **1964**, *40*, 1105.
- (20) Schatz, G. C. *Chem. Phys. Lett.* **1983**, *94*, 183.
- (21) Schatz, G. C.; Hubbard, L. M.; Dardi, P. S.; Miller, W. H. *J. Chem. Phys.* **1984**, *81*, 231.
- (22) Hubbard, L. M.; Shi, S. H.; Miller, W. H. *J. Chem. Phys.* **1983**, *78*, 2381.
- (23) Sato, S. *J. Chem. Phys.* **1955**, *23*, 592.
- (24) Johnson, B. R.; Winter, N. W. *J. Chem. Phys.* **1977**, *66*, 4116.

approximate theories against accurate results for series of isotopically related reactions in the full three-dimensional world (earlier tests were limited to the collinear world^{3-6,14,25} or to a single deuterated example¹⁴), and to provide a benchmark in these comparisons, we also test the predictions of conventional transition state theory (TST). TST has provided the standard theoretical framework for interpreting KIEs,²⁶ and there has been much recent interest in this kind of application.^{10,27,28} Since both VTST/G and TST methods are applicable even for large polyatomic systems, tests against accurate quantal results that can be obtained practically only for atom-diatom cases are of general practical interest.

II. Variational Transition State Theory Methods

Because of the importance of tunnelling in these reactions, the present comparisons will primarily test the accuracy of the transmission coefficient used in VTST/G calculations. We will study two approximations to this transmission coefficient, one based on the small-curvature-tunnelling semiclassical approximation²⁹ for tunnelling governed by the adiabatic ground-state potential curve (SCTSAG) and the other based on the least action ground state method (LAG).⁶ An important element in any multidimensional semiclassical tunnelling calculation is the way that the effects of reaction-path curvature are incorporated. When the reaction path through mass-scaled coordinates is curved, tunnelling fluxes tend to be dominated by tunnelling paths displaced to the concave side of the minimum energy path (MEP).³⁰ A kinematic indicator of the magnitude of the reaction-path curvature is the skew angle, defined as the angle between the entrance and exit valleys of the reactive potential energy surface in mass-scaled coordinates.⁶ Small skew angles generate large reaction path curvature and large deviations of optimum tunnelling paths from the MEP, whereas large-skew-angle systems may have smaller reaction-path curvature and can often be treated adequately by the small-curvature approximation.^{6,29} For the reactions R1-R7, the skew angle ranges from 36° for O + HD to 71° for H + DH. Thus a range of curvatures will be considered, and for some of these the small-curvature approximation, i.e., SCTSAG, may be inadequate. The LAG method, on the other hand, should be able to describe both the small- and large-curvature limits correctly and thus might be expected to be generally more accurate. Both the LAG and SCTSAG tunnelling factors are combined with a VTST rate coefficient obtained from improved canonical variational theory (ICVT), which is VTST for a canonical ensemble but enforcing the correct microcanonical threshold.³ Alternative VTST rate expressions^{3,7} would change the rate constants by negligible amounts relative to the ICVT ones for the reactions considered. The vibrational partition functions have been calculated by using a quadratic-quartic approximation for the bend³¹ and either the Morse I²⁵ (H + H₂ and isotopic analogues) or WKB¹¹ (O + H₂ and isotopic analogues) approximation for the stretch. The influence of the choice of stretch

eigenvalue method is small for these reactions, but past experience suggests that the WKB based results should be slightly more accurate. For reactions R4-R7, the multiple-electronic surface coefficient^{8,32} was set equal to $3/Q_{el}^R$ where the numerator is the electronic degeneracy of the lowest energy potential surface and the denominator is the electronic partition function of O. For reactions R1-R3, the multiple electronic surface coefficient was set equal to unity.

In addition to the VTST/G calculations, we performed conventional TST calculations, both without a transmission coefficient (these calculations are denoted \mp) and with the lowest order Wigner quantal correction for the reaction coordinate (these calculations are denoted \mp/W). These calculations are performed by standard methods reviewed elsewhere³³ and employ the same treatments of anharmonicity and multiple electronic surfaces as mentioned above.

III. Accurate Quantum Calculations

The CS calculations for reactions R1-R3 used the propagation/matching procedure presented previously³⁴ with the CS approximation of ref 20. In these calculations, the D + H₂, H + HD, and H + DH reactions are all studied in the same calculation, corresponding to different parts of the scattering matrix. H + H₂ is studied in a separate CS calculation. Only the $\Omega = 0$ projection quantum number is used in the CS basis, as the contribution of excited bending states to the rate constant at 300 K is negligible. Other Ω 's and higher temperatures could have been included of course but were not because poor convergence of the $\Omega = 0$ calculations for reactions R2 and R3 at total energies above 0.6 eV made it impractical to obtain reliable rate constants above 300 K for these reactions.

The accuracy of the CS rate constants may be assessed by comparison with the results of CC calculations³⁵ that have been done on H + H₂. The CC distinguishable-atom rate constants at 200, 250, and 300 K are 1.6×10^{-17} , 1.7×10^{-16} , and 9.8×10^{-16} cm³ molecule⁻¹ s⁻¹, respectively, while the corresponding CS values are 1.7×10^{-17} , 1.8×10^{-16} , and 1.0×10^{-15} cm³ molecule⁻¹ s⁻¹. These differ by 6% or less, suggesting that the CS approximation introduces negligible additional error since the CC thermally averaged rate constants, which are in principle exact, are claimed³⁵ to be numerically converged only to within 30%. Comparisons of reagent state resolved CC and CS cross sections generally indicate somewhat larger differences, up to 25%.²⁰ Because the numerical approximations introduced in doing the thermal averages for the present study add an additional 10% uncertainty, it is probably more realistic to use 35% as the estimated uncertainty in the CS rate constants.

The CSDW calculations on reactions R4-R7 have been extensively described elsewhere.² Although there have not yet been comparisons of CSDW and CS or CC rate constants for these reactions, comparisons of CSDW and CS cross sections for H + H₂ suggest that as long as the CSDW calculation can be and is converged with respect to basis set, the CSDW and CS results are essentially the same.³⁶ In the present case, convergence was excellent up to total energies of 0.7 eV for all four reactions. Since the 300 K rate constants are nearly converged at that energy, these should be as accurate as our CS rate constants. By adding partially converged cross sections at 0.8 and 1.0 eV, rate constants up to 500 K have been obtained. We will use these here although we are less confident in their absolute accuracy.

IV. Results

The results will be presented in two different ways for each set of isotopically related reactions. First, for reactions R1-R3, in Table I we present the ratios of various transition state theory and variational transition state theory rate constants to CS ones

(25) Garrett, B. C.; Truhlar, D. G. *J. Phys. Chem.* **1979**, *83*, 1079. Errata: *Ibid.* **1980**, *84*, 682; **1983**, *87*, 4553. Garrett, B. C.; Truhlar, D. G.; Grev, R. S.; Magnuson, A. W.; Connor, J. N. L. *J. Chem. Phys.* **1980**, *73*, 1721.

(26) Melander, L.; Saunders, W. H., Jr. "Reaction Rates of Isotopic Molecules"; 2nd ed.; Wiley: New York, 1980.

(27) Kreevoy, M. M.; Truhlar, D. G. In "Techniques of Chemistry", 4th ed.; Weissberger, A., Bernasconi, C. F., Eds.; Wiley: New York, 1986; Vol. 6, Part 1, p 13.

(28) For recent examples see: (a) Schatz, G. C.; Wagner, A. F.; Dunning, T. H., Jr. *J. Phys. Chem.* **1984**, *88*, 221. (b) Strong, H. L.; Brownawell, M. L.; San Filippo, J., Jr. *J. Am. Chem. Soc.* **1983**, *105*, 6526. (c) Ostovic, D.; Roberts, R. M. G.; Kreevoy, M. M. *J. Am. Chem. Soc.* **1983**, *105*, 7629. (d) Fujisaki, N.; Ruf, A.; Gaumann, T. *J. Chem. Phys.* **1984**, *80*, 2570. (e) Stein, R. L.; Fujihara, H.; Quinn, D. M.; Fischer, G.; Kullertz, G.; Barth, A.; Schowen, R. L. *J. Am. Chem. Soc.* **1984**, *106*, 1457. (f) Canadell, E.; Olivella, S.; Poblet, J. M. *J. Phys. Chem.* **1984**, *88*, 3545.

(29) Skodje, R. T.; Truhlar, D. G.; Garrett, B. C. *J. Chem. Phys.* **1982**, *77*, 5955.

(30) Marcus, R. A. *J. Chem. Phys.* **1966**, *45*, 4493; **1969**, *49*, 2617. Kuppermann, A.; Adams, J. T.; Truhlar, D. G. *Abstr. Pap. Int. Conf. Phys. Electron At. Collisions* **1973**, 149. Marcus, R. A.; Coltrin, M. J. *J. Chem. Phys.* **1977**, *67*, 2609. Kuppermann, A. *Theor. Chem. Adv. Perspectives* **1981**, *6A*, 80.

(31) Garrett, B. C.; Truhlar, D. G. *J. Phys. Chem.* **1979**, *83*, 1915.

(32) Truhlar, D. G. *J. Chem. Phys.* **1972**, *56*, 3189; **1974**, *61*, 440(E).

(33) Garrett, B. C.; Truhlar, D. G. *J. Chem. Phys.* **1980**, *72*, 3460.

(34) Kuppermann, A.; Schatz, G. C.; Baer, M. *J. Chem. Phys.* **1976**, *65*, 4596. Schatz, G. C.; Kuppermann, A. *J. Chem. Phys.* **1976**, *65*, 4642.

(35) Schatz, G. C.; Kuppermann, A. *J. Chem. Phys.* **1976**, *65*, 4668.

(36) Schatz, G. C. *Theory of Chemical Reaction Dynamics*; Clary, D. C., Ed.; Proceedings of NATO Workshop, Orsay, France, 1985, to be published.

Table I. Rate Constant Results for H + H₂, D + H₂, H + HD, and H + DH

T, K	ratio to CS rate constant					CS rate constant ^a
	‡	‡/W	ICVT	ICVT/SCTSAG	ICVT/LAG	
(A) H + H ₂ → H ₂ + H (Distinguishable Atoms)						
200	0.0018	0.021	0.0018	0.38	0.74	1.6 (-17) ^b
250	0.014	0.11	0.014	0.51	0.87	1.7 (-16)
300	0.044	0.25	0.044	0.60	0.92	1.0 (-15)
(B) D + H ₂ ↔ DH + H						
200	0.0035	0.036	0.0033	0.27	0.57	2.6 (-17) ^c
250	0.021	0.15	0.021	0.39	0.69	2.6 (-16) ^c
300	0.060	0.31	0.058	0.47	0.74	1.4 (-15) ^c
(C) H + DH → HD + H (Distinguishable Atoms)						
200	0.0040	0.031	0.0040	0.97	1.03	1.2 (-18)
250	0.029	0.16	0.029	1.17	1.10	1.5 (-17)
300	0.086	0.35	0.086	1.22	1.07	1.1 (-16)

^aIn cm³ molecule⁻¹ s⁻¹. ^bNumbers in parentheses are powers of ten. ^cForward (D + H₂) rate constant.

Table II. CS and VTST Kinetic Isotope Effects for H + H₂, D + H₂, and H + HD/DH

T, K	‡	‡/W	ICVT	ICVT/SCTSAG	ICVT/LAG	CS
(A) D/H ^a						
200	3.1	2.8	2.9	1.2	1.3	1.6
250	2.3	2.1	2.2	1.1	1.2	1.5
300	1.9	1.8	1.9	1.1	1.1	1.4
(B) H/(HD + DH)						
200	2.6	3.1	2.6	3.6	5.0	5.3
250	2.2	2.7	2.3	3.0	4.1	4.0
300	2.0	2.4	2.1	2.7	3.5	3.2
(C) D/(HD + DH)						
200	7.9	8.7	7.7	4.2	6.3	8.4
250	5.2	5.7	5.1	3.4	4.8	6.0
300	3.9	4.3	3.9	2.9	3.9	4.5
(D) HD/DH						
200	1.4	1.8	1.3	0.45	0.87	1.7
250	1.4	1.8	1.3	0.62	1.2	2.0
300	1.4	1.7	1.3	0.76	1.4	1.8

^aSee section IV for labeling convention for kinetic isotope effects.

Table III. Rate Constant Results for O + H₂, D₂, HD, and DH

T, K	ratio to CS rate constant					CS rate constant ^a
	‡	‡/W	ICVT	ICVT/SCTSAG	ICVT/LAG	
(A) O + H ₂ → OH + H						
300	0.053	0.25	0.052	0.87	1.28	1.1 (-17) ^b
400	0.16	0.51	0.16	0.91	1.11	2.9 (-16)
500	0.30	0.70	0.29	0.95	1.06	2.3 (-15)
(B) O + D ₂ → OD + D						
300	0.14	0.42	0.14	1.29	1.00	6.9 (-19)
400	0.30	0.62	0.30	1.09	0.83	3.7 (-17)
500	0.44	0.74	0.44	1.03	0.82	4.5 (-16)
(C) O + HD → OH + D						
300	0.085	0.37	0.085	0.64	1.22	2.0 (-18)
400	0.21	0.60	0.21	0.71	1.09	7.3 (-17)
500	0.33	0.74	0.33	0.77	1.04	7.0 (-16)
(D) O + DH → OD + H						
300	0.15	0.48	0.14	1.47	0.91	7.3 (-19)
400	0.39	0.86	0.36	1.41	0.92	2.7 (-17)
500	0.64	1.14	0.61	1.48	1.06	2.6 (-16)

^aIn cm³ molecule⁻¹ s⁻¹. ^bNumbers in parentheses are powers of tens.

at three temperatures (200, 250, and 300 K) where the CS result should be accurate. The ratios for reactions R2a and R2b are the same because of microscopic reversibility. Included in the table are results from conventional transition state theory (‡), Wigner-corrected conventional transition state theory (‡/W), improved canonical variational theory (ICVT), ICVT with small-curvature-tunnelling semiclassical adiabatic ground-state transmission coefficients (ICVT/SCTSAG), and ICVT with least-action ground-state transmission coefficients (ICVT/LAG). For reference, in Table I we also present the absolute rate constants from ref 1, each one referring to a distinguishable-atom model

of the reagent diatomic. Table II presents an alternative way to analyze the results in Table I through an evaluation of the kinetic isotope effects, i.e., the rate constant isotope ratios D + H₂/H + H₂, H + H₂/((H + HD) + (H + DH)), D + H₂/((H + HD) + (H + DH)), and H + HD/H + DH, where we have used the convention that A + HD refers to A + HD → AH + D and A + DH refers to A + DH → AD + H. We abbreviate these ratios by D/H, H/(HD + DH), D/(HD + DH), and HD/DH, respectively.

Tables III and IV present results analogous to those in Tables I and II but for reactions R4–R7. Here the isotope ratios refer

Table IV. CSDW and VTST Kinetic Isotope Effects for O + H₂, D₂, HD, and DH

T, K	‡	‡/W	ICVT	ICVT/SCTSAG	ICVT/LAG	CSDW
(A) H ₂ /D ₂ ^a						
300	5.81	9.48	5.72	10.7	20.4	15.6
400	4.30	6.44	4.25	6.50	10.4	7.7
500	3.49	4.85	3.46	4.71	6.62	5.0
(B) H ₂ /(HD + DH)						
300	2.06	2.51	2.08	4.05	4.53	4.0
400	1.86	2.20	1.87	2.91	3.07	2.9
500	1.72	1.98	1.73	2.37	2.44	2.4
(C) (HD + DH)/D ₂						
300	2.81	3.78	2.75	2.64	4.50	3.9
400	2.31	2.93	2.27	2.23	3.39	2.7
500	2.03	2.45	1.99	1.99	2.72	2.1
(D) HD/DH						
300	1.52	2.12	1.64	1.18	3.67	2.7
400	1.44	1.89	1.53	1.36	3.19	2.7
500	1.38	1.73	1.47	1.40	2.65	2.7

^aSee section IV for labeling convention for kinetic isotope effects.

to O + H₂/O + D₂, O + H₂/((O + HD) + (O + DH)), ((O + HD) + (O + DH))/O + D₂, and O + HD/O + DH and are respectively abbreviated H₂/D₂, H₂/(HD + DH), *(HD + DH)/D₂, and HD/DH.

V. Discussion

The ‡ and ‡/W results are used to assess the accuracy of commonly used approximate theories. Both the ‡ and ICVT models correspond to classical reaction-coordinate motion and quantized vibrational-rotational motions but differ as to whether the location of the generalized transition state is variationally optimized. Thus reference to these two results provides an indication of the importance of tunnelling when compared to accurate or ICVT/G rate constants. Table I indicates that the ‡ and ICVT results are nearly the same for the H + H₂ reaction and all three isotopic analogues, indicating that variational effects (i.e., differences due to variational location of the generalized transition state somewhere other than the saddle point) are not important. (See ref 25, 33, and 37 for earlier discussions of this point for the H₃ isotopes.) These methods are not in good agreement with the accurate results though, indicating that tunnelling is very important. More detailed analysis of the LAG result shows that at 300 K tunnelling contributes 97% of the H + H₂ rate constant, 94% of the D + H₂ one, and 95% of the H + DH one. (These tunnelling fractions are computed as described elsewhere.²⁹) At 200 K, tunnelling increases the ICVT/LAG rate constants by factors of 555, 303, and 250, relative to ICVT, for these same reactions.

We turn now to the accuracy of the tunnelling-corrected ‡/W and VTST/G results. First we note that the Wigner-corrected results are low for all four reactions, by factors of 3–4 at 300 K and 30–50 at 200 K. The ICVT/SCTSAG and ICVT/LAG results are much more accurate, with the LAG ones being noticeably better than the SCTSAG ones for H + H₂ and especially D + H₂. The LAG result is within the 35% uncertainty of the CS rate constant for H + H₂ and H + DH but not for D + H₂ at low temperatures. However, the worst error in the LAG rate constants for D + H₂ over the whole temperature range considered is only 43%. The worst error in the SCTSAG rate constants is also for D + H₂, for which it is 73% at 200 K. The SCTSAG method does best for the reaction with the largest skew angle, H + DH; this aspect of the results is consistent with the fact that the SCTSAG method assumes small curvature of the reaction path.

Turning now to the isotope ratios in Table II, we note that the D/H and H/(HD + DH) ratios are strongly influenced by tunnelling. For example, at 250 K, the ICVT D/H ratio is 2.2, but the ICVT/LAG approximation reduces this to 1.2 and the CS

value is 1.5. For H/(HD + DH) at 250 K, ICVT predicts the value 2.3, but the ICVT/LAG approximation raises this to 4.1 and the CS value is 4.0. The D/(HD + DH) and HD/DH ratios, by contrast, are not as strongly influenced by tunnelling, with the ICVT and ICVT/LAG results within 10% of each other.

The comparison of VTST/G and CS isotope ratios generally reflects trends seen in Table I. Thus, since ICVT/LAG underestimates the D + H₂ rate constant but is very close for H + H₂, the LAG D/H ratio is below the CS result by ~20%. Since the LAG rate constant is lower than the CS one for H + HD, but slightly higher for H + DH, the HD + DH summed rate constant is slightly lower than the CS result, making the H/(HD + DH) ratio essentially perfect and D/(HD + DH) slightly low. The worst comparison of LAG and CS isotope ratios is for the HD/DH ratio. This reflects the fact that the H + HD rate constant is too low while the H + DH one is slightly high, leading to a HD/DH ratio which is too low by 22–49%. The ICVT/LAG isotope ratios are in better agreement with CS results than are the ‡, ‡/W, and ICVT ratios for D/H and H/(HD + DH). For D/(HD + DH) and HD/DH, where tunnelling has less effect on the ratio, the ‡, ‡/W, and ICVT ratios are generally of comparable accuracy to ICVT/LAG. The ICVT/SCTSAG results are generally less accurate than the ICVT/LAG ones, although the differences are quite small except for HD/DH. The latter ratio is especially poor when SCTSAG is used because the H + HD rate constant is very low while H + DH is essentially perfect. This result suggests that one should be cautious in using SCTSAG to predict intramolecular isotope effects when there is a substantial difference in curvature between the two competing arrangement channels.

Turning to reactions R4–R7, we see in Table III that the ‡ and ICVT results are in good agreement with each other but are very different from the tunnelling corrected results. This suggests that, as for reactions R1–R3, variational effects are small while tunnelling contributions to the rate constants are large. Among the tunnelling corrected rate constants, the ICVT/LAG rate constants are in overall best agreement with accurate quantum ones, with differences that show no significant isotope dependence (to within about ±30%). The ICVT/SCTSAG results are also quite accurate, though usually less so than the ICVT/LAG results. The least accurate SCTSAG results are for O + HD and DH, which show trends somewhat like H + HD and H + DH in that the SCTSAG rate constants for the smaller-skew-angle reaction are below the accurate results while those for the larger-skew-angle reaction are too high. However, unlike the H + HD/DH case, the error for the larger-skew-angle reaction is as large as that for the small-skew-angle reaction. This is not surprising, however, since O + DH has a larger skew angle than O + H₂ or O + D₂ and SCTSAG does sometimes overestimate the tunnelling for the largest skew angles.⁶ Also, the differences between the SCTSAG and LAG rate constants are quite large for O + DH, suggesting that curvature effects are substantially larger for O + DH than

(37) Miller, W. H. *Potential Energy Surfaces and Dynamics Calculations*; Truhlar, D. G., Ed.; Plenum: New York, 1981; p 265.

for H + DH where the SCTSAG and LAG rate constants are essentially the same.

Note that the ICVT/LAG results are better than \mp/W for all four reactions R4-R7 over the temperatures considered. This is consistent with studies of the collinear O + H₂ reaction for five potential energy surfaces,⁸ on which basis, it was concluded that the LAG transmission coefficient provides an accurate method for describing tunnelling in this case.

Table IV shows that the ICVT/LAG isotope effects are in good agreement with the CSDW ones for all four ratios; the worst difference is 38%. The ICVT/SCTSAG method also does well except for HD/DH where the direction of the error is opposite that of the ICVT/LAG results. Considering the \mp/W isotope ratios, we see that the \mp/W approximation does much better in predicting isotope ratios than absolute rate constants. For (HD + DH)/D₂, the cancellation of errors in the \mp/W ratios is usually better than for the ICVT/SCTSAG or ICVT/LAG ratios, but for the other ratios it is not.

As stated in the introduction, the goal of this study has been to compare approximate rate constants and kinetic isotope effects to accurate dynamical ones for the same potential energy surface rather than to experiment. We have found that the approximate VTST/G rate constants are indeed quite reliable, and we conclude that comparisons of calculations based on more accurate potential energy surfaces to experiment for these systems^{5,8,13,33,38,39} may be interpreted in terms of the accuracy of the potential energy surfaces and the experiments, with relatively much less possible error attributable to the dynamical treatment. Since the potential surfaces employed for this study are typical medium-barrier-height surfaces, the conclusion is assumed to be generalizable.

VI. Conclusions

For six of the seven independent reactions considered in this study, the ICVT/LAG rate constants agree with accurate quantum rate constants at all the temperatures considered to within the estimated (35%) uncertainty of the quantum rate constants. The only exception is the D + H₂ \leftarrow H + HD reaction, for which the ICVT/LAG rate constants differ from the numerical quantal dynamical ones by 43% at 200 K. Kinetic isotope effects are also

accurately predicted by the ICVT/LAG approximation, with the worst results occurring for intramolecular (X + HD) isotope ratios. The ICVT/SCTSAG rate constants are generally less accurate than the ICVT/LAG ones, with the worst error being 73%. Considering all seven reactions at all temperatures studied, the average errors for the ICVT/LAG and ICVT/SCTSAG rate constants are only 15% and 31%, respectively. Since all of these reactions have tunnelling factors larger than about 5 at the temperatures studied, these comparisons demonstrate the remarkable accuracy of the LAG and SCTSAG methods for determining tunnelling factors. Simple theories like conventional TST, with or without a Wigner tunnelling correction, are found to be grossly in error for predicting the rate constants of these reactions and usually less accurate in predicting isotope ratios.

We can summarize the overall accuracy of the ICVT/LAG method for all nine reactions for which comparisons to accurate quantal results are available by combining the present results with those of ref 11, 13, 14, and 35. The only temperature for which comparisons are possible for all nine cases is 300 K. At this temperature, the average discrepancy between the ICVT/LAG results and the accurate quantal ones is only 12%. Furthermore, in only one case is the discrepancy larger than 26%. For the reactions involved in the comparison, the error is expected to decrease as the temperature is increased because most of the error at 300 K is probably caused by inaccuracies in the semiclassical transmission probabilities for energies below the effective barrier, and these become less important as the temperature is increased. Thus the accuracy attained is very encouraging, especially since variational transition state theory with semiclassical ground-state transmission coefficients is a practical theory for a wide range of systems, including reactions of polyatomics for which more accurate methods are impractical.

Acknowledgment. The research at Northwestern University (GCS) was supported by a grant from the National Science Foundation (CHE-8416026). Research at Chemical Dynamics Corporation was supported by the United States Army Research Office under contract Number DAAG 29-84-C-0011. Research at the University of Minnesota was supported by the U.S. Department of Energy, Office of Basic Energy Sciences, under contract DE-ACO2-79ER10425.

Registry No. H, 12385-13-6; H₂, 1333-74-0; D, 16873-17-9; HD, 13983-20-5; O, 17778-80-2; D₂, 7782-39-0.

(38) Blais, N. C.; Truhlar, D. G.; Garrett, B. C. *J. Phys. Chem.* **1981**, *85*, 1094; *J. Chem. Phys.* **1982**, *76*, 2768; **1983**, *78*, 2363.

(39) Garrett, B. C.; Truhlar, D. G. *Int. J. Quantum Chem.*, in press.

Intrinsic Reactivity of Magnesium Surfaces toward Methyl Bromide

Ralph G. Nuzzo* and Lawrence H. Dubois*

Contribution from AT&T Bell Laboratories, Murray Hill, New Jersey 07974.

Received October 16, 1985

Abstract: The chemisorption and subsequent decomposition of methyl bromide on a Mg(0001) single-crystal surface is found to lead cleanly to the formation of a surface bromide and gas-phase hydrocarbon products including ethane. Stable surface alkyls are not observed even at temperatures as low as -150 °C. Co-adsorbed dimethyl ether does not perturb this reactivity pattern. The formation of either a thin surface bromide or a surface oxide passivates this material to further reaction under UHV conditions. The implications of these results with respect to the mechanisms of carbon-halogen bond cleavage on magnesium and the formation of Grignard reagents are discussed.

There is perhaps no general class of organometallic reactions that rivals in importance the reductive cleavage of carbon-halogen bonds by active metals.¹ Of the many examples of this type of process that one could cite, none assumes the synthetic and his-

torical stature of the formation of the Grignard reagent. The reactivity of these complexes has been studied extensively and, as a result, there is much known about the application of these reagents in synthesis.^{1,2} Reliable information about the mech-

(1) Coates, G. E.; Green, M. L. M.; Wade, K. *Organometallic Compounds. Volume 1. The Main Group Elements*, Methuen and Co.: London, 1967; and references cited therein.

(2) See, for example: Kharasch, M. S.; Reinnuth, O. *Grignard Reactions of Nonmetallic Substances*; Prentice-Hall: New York, 1954; and references cited therein.